Title
Diffraction at a thick screen including corrugations on the top face

Journal
IEEE Transactions on Antennas and Propagation, 45(2)

ISSN
0018-926X

Authors
Albani, M
Capolino, F
Maci, S
et al.

Publication Date
1997-12-01

DOI
10.1109/8.560346

Diffraction at a Thick Screen Including Corrugations on the Top Face

Matteo Albani, Filippo Capolino, *Student Member, IEEE*, Stefano Maci, *Member, IEEE*, and Roberto Tiberio, *Fellow, IEEE*

***Abstract*—A closed-form high-frequency solution is presented for the near-field scattering by a thick screen illuminated by a line source at a finite distance. This solution is applicable to a thick screen with perfectly conducting side walls and either perfectly conducting or artificially soft boundary conditions on the face joining the two wedges. This latter condition is obtained in practice by etching on that face quarter of a wavelength deep corrugations with a small periodicity with respect to the wavelength. It is shown that the artificially soft surface provides a strong shadowing for both polarizations; thus, it is suggested that such configurations may usefully be employed to obtain an effective shielding from undesired interferences. Several numerical calculations have been carried out and compared with those from a method of moments (MoM) solution for testing the accuracy of our formulation, as well as to demonstrate the effectiveness of the corrugations in shielding arbitrarily polarized incident field.**

***Index Terms*—Geometrical theory of diffraction.**

I. Introduction

ELECTROMAGNETIC interference between antennas and/or apparatuses operating in a constrained environment is a problem of increasing importance, especially for overcrowded space platforms. One of the most simple but effective ways to reduce the interference is to separate the apparatuses by introducing barriers between them. This solution can also be useful in reducing interference in earth satellite stations. Indeed, limited spectrum availability often results in disturbances owing to the frequency sharing of radio communication signals [1]. Interferences that arise from microwave links operating at the same frequency often arrive from directions close to the horizon; they may sometimes be attenuated by diffraction losses at natural barriers occurring in terrain propagation. In other cases, introducing artificial shielding barriers may greatly alleviate these problems.

The simplest canonical model of a barrier for interference protection is a perfectly conducting thick screen of a semi-infinite extent. When the source and the observer are optically shadowed, a field coupling still occurs due to double diffraction (DD) mechanisms at the two nearby parallel edges of the screen. Consequently, its shielding effectiveness significantly depends upon the thickness and the polarization of the incident field. In particular, when the incident electric field is parallel to the edges (E_z-pol soft-boundary condition), the diffracted field into the shadow region is very weak, since the first-order diffracted field is short circuited by the conducting portion between the two edges. Then, the second-order diffraction essentially consists of a slope effect, that becomes weaker as the thicknesses increases.

On the other hand, when the incident electric field is perpendicular to the edges (H_z-pol hard-boundary condition), a stronger field penetrates into the shadow region because the first-order diffracted field does not vanish between the two edges. This results in poor shielding. To improve the shielding effectiveness for this polarization, one can etch in the face, joining the two edges quarter of a wavelength, deep corrugations with a small periodicity with respect to the wavelength. For such configurations, the surface at the top of the corrugations may be appropriately modeled as a perfectly magnetic conducting (pmc) surface for the H_z-pol and a perfectly electric conducting (pec) surface for the E_z-pol; thus, an artificially soft boundary condition (BC) is obtained [2], which leads to a similar behavior of the field for both polarizations.

In this paper, a closed-form high-frequency solution is derived, for a thick screen with pec side walls, and either pec or artificially soft BC on the face between the two edges. The high-frequency description of DD mechanisms at a pair of interacting edges has been thoroughly considered in the literature [3]–[12]. As is rather well known, this problem cannot be approached by using successive applications of the ordinary uniform geometrical theory of diffraction (UTD) diffraction coefficients [13]; indeed, this procedure fails when the second edge is located in the transition region of the first edge and the diffracted field is calculated close to and at the shadow (SB) or reflection (RB) boundary of the second edge. This is due to the rapid spatial variation and the nonray-optical behavior of the incident field at the second edge after diffracting from the first. The problem of diffraction by two parallel edges was first investigated in [3]–[5]. In [5], the analysis was restricted to SB (RB) fields from the second edge. In [6] and [7], this restriction was removed by different formulations to provide diffraction coefficients for plane wave incidence and far-field observation. A different formulation for the same problem was developed in [7]. A different approach based on the physical theory of diffraction (PTD) was pursued in [8] and [9]. Within this same framework significant improvements were given in [10] and [11], where the problem of skewed, coplanar wedges was analyzed. In this

Manuscript received April 9, 1996; revised July 3, 1996.

F. Capolino and S. Maci are with the Department of Electronics Engineering, University of Florence, Florence, 50139, Italy.

M. Albani and R. Tiberio are with the College of Engineering, University of Siena, Siena, 53100, Italy.

Publisher Item Identifier S 0018-926X(97)01452-X.

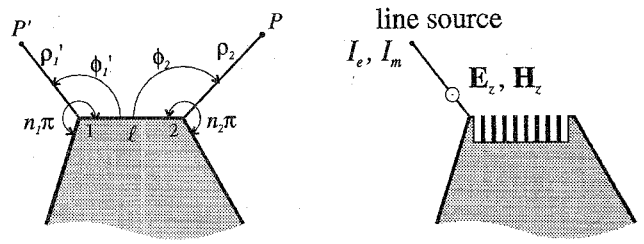

Fig. 1. Geometry at the thick screen. (a) *pec* smooth screen. (b) Artificially soft corrugated screen illuminated by a line source. Both TE_z (magnetic line source) and TM_z (electric line source) are considered.

paper, an extended UTD closed-form solution [12] is presented for describing DD mechanisms in the near zone of the edges of thick-screen configurations (as those described above) when they are illuminated by a line source.

The DD analysis which is formulated in Section II consists of two steps. First, the cylindrical wave spectrum of the diffracted field from the first wedge [13] is used as the incident field at the second wedge. For the case of corrugations, the spectral solution presented in [14] and [15] is used which is relevant to a wedge with *pec* BC on one face and artificially soft BC on the other face. Next, the near-field response of the second edge to each cylindrical spectral source is used to obtain a double-integral representation for the doubly diffracted field [6]. In Section III, this integral is asymptotically evaluated to find the desired closed-form (ray-optical) expressions. This asymptotic evaluation leads to transition functions involving generalized Fresnel integrals (GFI) [16], [17]. Numerical results are presented in Section IV, where our solution is validated against a method of moments (MoM) analysis of both smooth and corrugated screens. In this same section, the shielding effectiveness of the corrugated screen is discussed; it is also shown that when the screen thickness decreases, our solution fails so gracefully that it even recovers the field of a half-plane for vanishing thickness.

II. Formulation

The geometry of the thick screen without corrugations is shown in Fig. 1(a). Two parallel axes z_i are defined along the two edges and a cylindrical coordinate system (ρ_i, ϕ_i) is introduced at each edge $i = 1, 2$; $n_i\pi$ denotes the exterior wedge angle at each edge and ℓ the thickness of the screen. A uniform either electric (TM_z) or magnetic (TE_z) line-source illumination is assumed. A quarter of a wavelength corrugated screen is also considered [Fig. 1(b)] that is modeled by an artificially soft BC at the top of the corrugations (i.e., *pec* for TM_z and *pmc* for TE_z illumination). For the corrugated screen, only the TE_z illumination is considered because the TM_z solution is the same for both cases within the approximation of artificially soft surface.

Let us denote by $P'(\phi_1') \equiv (\rho_1', \phi_1')$ the source point; its incident field at any point $P(\phi_1) \equiv (\rho_1, \phi_1)$ is

$$\psi[P(\phi_1), P'(\phi_1')] = \frac{1}{4j} H_0^{(2)}(k|P(\phi_1) - P'(\phi_1')|) \quad (1)$$

which represents either the normalized $jE_z/k\zeta I_e$ electric field for an electric line source (TM_z) or $j\zeta H_z/kI_m$ magnetic field for a magnetic line source (TE_z). A $e^{j\omega t}$ time dependence is assumed and suppressed. The total field is represented as the sum of the geometrical optics (GO) field plus singly diffracted fields from edges 1 and 2 and doubly diffracted fields.

Our description of the DD mechanism is constructed as the superposition of two analogous mechanisms—a diffracted field from edge 2 when it is illuminated by the diffracted field from edge 1 (ψ_{12}^{dd}), and that from edge 1 when it is illuminated by edge 2 (ψ_{21}^{dd}). In the following, contribution 12 is explicitly considered; it is then a straightforward matter to obtain the corresponding expression for contribution 21. The scalar diffracted field from edge 1 at any point $P(\phi_1)$ is conveniently represented as [18]

$$\psi_1^d[P(\phi_1), P'(\phi_1')] = \frac{1}{2\pi j} \int_{C_{\alpha_1}} \psi[P(\phi_1), P'(\alpha_1 \pm \pi)] \cdot G_1(\phi_1', \alpha_1)\, d\alpha_1 \quad (2)$$

where the $\pm$ sign applies to $\phi_1 \lessgtr \pi$, the contour of integration C_{α_1} is defined along $(-j\infty, \pi + j\infty)$, and a clockwise indentation around the relevant GO pole is assumed. The G_1 function is conveniently expressed as [14]

$$G_1(\phi_1', \alpha_1) = -\sum_{p=1}^{2} (-1)^p F_1^{h,a,s}(\Phi_1^p, \alpha_1) \quad (3)$$

where $\Phi_1^p = \phi_1' + (-1)^p\pi$, and the superscripts h, a refer to the TE_z polarization for hard and artificially soft BC, respectively, and s to the TM_z polarization for both configurations. In (3)

$$F_i^{h,a,s}(\Phi, \alpha) = \frac{1}{n_i} \frac{f_i^{h,a,s}(\Phi, \alpha)}{\cos\dfrac{\alpha}{n_i} - \cos\dfrac{\Phi}{n_i}} \quad (4)$$

in which

$$f_i^h(\Phi, \alpha) = \sin\frac{\Phi}{n_i} \quad (5)$$

$$f_i^a(\Phi, \alpha) = 2\cos\frac{\Phi}{2n_i} \sin\frac{\alpha}{2n_i} \quad (6)$$

$$f_i^s(\Phi, \alpha) = \sin\frac{\alpha}{n_i}. \quad (7)$$

The integrand in (2) is interpreted as the field of spectral line sources localized at $P'(\alpha_1 \pm \pi) \equiv (\rho_1', \alpha_1 \pm \pi)$. Then, these sources are used to illuminate the second wedge. Thus, each line source provides a diffracted field contribution from wedge 2 at any point $P(\phi_2) \equiv (\rho_2, \phi_2)$. For the sake of convenience, this contribution is calculated by invoking reciprocity (i.e., by calculating the diffracted field from wedge 2 at $P'(\alpha_1 \pm \pi)$ due to a line source at $P(\phi_2)$). This procedure leads to

$$\psi_2^d[P(\phi_2), P'(\alpha_1 \pm \pi)] = \frac{1}{2\pi j} \int_{C_{\alpha_2}} \psi[P'(\alpha_1 \pm \pi), P(\alpha_2 \pm \pi)] G_2(\phi_2, \alpha_2) d\alpha_2 \quad (8)$$

in which $P(\alpha_2 \pm \pi) \equiv (\rho_2, \alpha_2 \pm \pi)$, the contour C_{α_2} is the same as C_{α_1}, and

$$G_2(\phi_2, \alpha_2) = -\sum_{q=1}^{2} (-1)^q F_2^{h,a,s}(\Phi_2^q, \alpha_2) \quad (9)$$

where $\Phi_2^q = \phi_2 + (-1)^q\pi$, and $F_2^{h,a,s}$ are the same as those in (4)–(7).

The spectral response of edge 2 is then described by the integrand of (2) after replacing therein $\psi[P(\phi_1), P'(\alpha_1 \pm \pi)]$ by $\psi_2^d[P(\phi_2), P'(\alpha_1 \pm \pi)]$. By spectral synthesis, the desired double spectral integral representation for the doubly diffracted field ψ_{12}^{dd} is obtained

$$\psi_{12}^{dd} = -\frac{1}{8\pi^2}\int_{-j\infty}^{j\infty}\int_{-j\infty}^{j\infty}\frac{1}{4j}H_0^{(2)}(kR(\alpha_1,\alpha_2)) \cdot G_1(\phi_1',\alpha_1)G_2(\phi_2,\alpha_2)\,d\alpha_1\,d\alpha_2 \tag{10}$$

in which the convenient notation (11), as shown at the bottom of the page, has been introduced to provide an explicit expression for $\psi[P'(\alpha_1 \pm \pi), P(\alpha_2 \pm \pi)]$ within the integral representation of ψ_2^d in (2). In (10), the original contours of integration have been deformed onto their imaginary axis and a 1/2 factor has been introduced to take into account that the two wedges share a common face [4]. Equation (10) explicitly satisfies reciprocity and is found suitable for asymptotic evaluation.

III. High-Frequency Solution

The double spectral integral representation for ψ_{12}^{dd} is now asymptotically evaluated to find a high-frequency expression for this DD mechanism. It is seen that the integral in (10) exhibits a two-dimensional (2-D) stationary phase point at $(\alpha_1, \alpha_2) = (0, 0)$. Its asymptotic contribution provides the doubly diffracted ray field. It is worth pointing out that in (10), the pole singularities of the spectra $G_1(\phi_1', \alpha_1)$ and $G_2(\phi_2, \alpha_2)$ independently occur in the two variables of integration. These poles may occur close to and at the stationary point; thus, they have to be appropriately accounted for in the asymptotic evaluation. The doubly diffracted field can be conveniently expressed as the sum of four integral terms

$$\psi_{12}^{dd} = -\frac{1}{4\pi^2}\sum_{p,q=1}^{2}(-1)^{p+q}\int_{-j\infty}^{j\infty}\int_{-j\infty}^{j\infty} \cdot \frac{1}{4j}H_0^{(2)}(kR(\alpha_1,\alpha_2)) \cdot F_1^{h,a,s}(\Phi_1^p,\alpha_1) \cdot F_2^{h,a,s}(\Phi_2^q,\alpha_2)\,d\alpha_1\,d\alpha_2 \tag{12}$$

and their uniform asymptotic evaluation is performed by taking into account the nearest poles to the saddle point. Thus, a pole singularity occurs in each relevant F_i function only at $\alpha_1 = \pm(\Phi_1^p - 2n_1N^p\pi)$ and $\alpha_2 = \pm(\Phi_2^q - 2n_2N^q\pi)$, where N^p, N^q are the integers that most nearly satisfy the relations

$$N^p = \frac{\Phi_1^p}{2n_1\pi}; \quad N^q = \frac{\Phi_2^q}{2n_2\pi}. \tag{13}$$

It is worth noting that the function F_i is either even or odd with respect to the integration variable for either hard (h) or soft/artificially soft (s/a) BC, respectively. Furthermore, it is seen that in these latter cases, the integrand vanishes at the saddle point, thus requiring a more involved asymptotic evaluation.

As shown in the Appendix, the following high-frequency solution for the DD mechanism 12 is obtained:

$$\psi_{12}^{dd} \sim \psi^i(O_1)\frac{e^{-jk(\ell+\rho_2)}}{\sqrt{\ell\rho_2}}D_{12}^{h,a,s} \tag{14}$$

where

$$\psi^i(O_1) = \frac{e^{-jk\rho_1'}}{2\sqrt{2\pi jk\rho_1'}} \tag{15}$$

which denotes either the incident E_z^i or H_z^i field at edge 1, in the TM_z or TE_z case, respectively. In (14) $D_{12}^{h,a,s}$ denote the double diffraction coefficients for the hard (h) and the artificially soft (a) cases, that apply to the TE_z polarization, and for the soft (s) case, that applies to the TM_z polarization. They are expressed as

$$D_{12}^h = \frac{1}{4\pi jk}\cdot\sum_{p,q=1}^{2}\frac{(-1)^{p+q}}{n_1n_2}\cot\left(\frac{\Phi_1^p}{2n_1}\right) \cdot\cot\left(\frac{\Phi_2^q}{2n_2}\right)\cdot\tilde{T}(a_p,b_q,w) \tag{16}$$

$$D_{12}^a = \frac{-1}{16\pi k^2\ell}\cdot\sum_{p,q=1}^{2}\frac{(-1)^{p+q}}{(n_1n_2)^2}\frac{\cos\left(\frac{\Phi_1^p}{2n_1}\right)}{\sin^2\left(\frac{\Phi_1^p}{2n_1}\right)} \cdot\frac{\cos\left(\frac{\Phi_2^q}{2n_2}\right)}{\sin^2\left(\frac{\Phi_2^q}{2n_2}\right)}\cdot\tilde{\tilde{T}}(a_p,b_q,w) \tag{17}$$

and

$$D_{12}^s = \frac{-1}{16\pi k^2\ell}\cdot\sum_{p,q=1}^{2}\frac{(-1)^{p+q}}{(n_1n_2)^2}\csc^2\left(\frac{\Phi_1^p}{2n_1}\right) \cdot\csc^2\left(\frac{\Phi_2^q}{2n_2}\right)\cdot\tilde{\tilde{T}}(a_p,b_p,w). \tag{18}$$

Equations (16)–(18) involve the transition functions

$$\tilde{T}(a,b,w) = \frac{2\pi jab}{\sqrt{1-w^2}}\left[\mathcal{G}\left(a,\frac{b+wa}{\sqrt{1-w^2}}\right)+\mathcal{G}\left(b,\frac{a+wb}{\sqrt{1-w^2}}\right) + \mathcal{G}\left(a,\frac{b-wa}{\sqrt{1-w^2}}\right)+\mathcal{G}\left(b,\frac{a-wb}{\sqrt{1-w^2}}\right)\right] \tag{19}$$

and

$$\tilde{\tilde{T}}(a,b,w) = \frac{-4\pi(ab)^2}{w\sqrt{1-w^2}}\left[\mathcal{G}\left(a,\frac{b+wa}{\sqrt{1-w^2}}\right) + \mathcal{G}\left(b,\frac{a+wb}{\sqrt{1-w^2}}\right)-\mathcal{G}\left(a,\frac{b-wa}{\sqrt{1-w^2}}\right) - \mathcal{G}\left(b,\frac{a-wb}{\sqrt{1-w^2}}\right)\right] \tag{20}$$

$$R(\alpha_1,\alpha_2) = \sqrt{\rho_1'^2+\ell^2+\rho_2^2+2\rho_1'\ell\cos\alpha_1+2\rho_2\ell\cos\alpha_2+2\rho_1'\rho_2\cos(\alpha_1+\alpha_2)} \tag{11}$$

where $\mathcal{G}$ is the GFI [16], [17]

$$\mathcal{G}(x,y) = \frac{y}{2\pi} e^{jx^2} \int_x^\infty \frac{e^{-j\tau^2}}{\tau^2 + y^2}\, d\tau \tag{21}$$

which can be easily calculated [19].

The distance parameters involved in the transition functions are

$$a_p = \sqrt{2k\frac{\rho_1'\ell}{\rho_1' + \ell}}\sin\left(\frac{\Phi_1^p - 2n_1 N^p \pi}{2}\right)$$
$$b_q = \sqrt{2k\frac{\rho_2\ell}{\rho_2 + \ell}}\sin\left(\frac{\Phi_2^q - 2n_2 N^q \pi}{2}\right) \tag{22}$$

and

$$w = \sqrt{\frac{\rho_1'\rho_2}{(\rho_1' + \ell)(\ell + \rho_2)}}. \tag{23}$$

It is rather apparent that the same overall process leading to the high-frequency equation (14) is applicable to find the corresponding equation for mechanism 21.

IV. Numerical Results

Several numerical calculation have been carried out to test the accuracy of the formulation presented here, as well as to demonstrate the effectiveness of the corrugations in shielding arbitrarily polarized fields. Calculations of the total field are shown in Fig. 2 for a thick screen with $\ell = \lambda/2$, when the observation point moves from the lit to the shadowed face as depicted in the inset. The line source is placed at a distance $\rho_1' = 2\lambda$ from the leading edge and 60° from the lit face of the screen. The results relevant to *pec* TE_z (h) and corrugated TE_z (a) cases, are plotted by dotted and continuous lines, respectively. The TM_z (s) case, is plotted by a dashed line. In the first region, ($\phi < 120°$) the TE_z responses for the corrugated and the smooth screens nearly overlap, as expected since the total field is dominated by the incident and reflected fields, that are the same for both cases. In the second region, ($150° < \phi < 290°$), soft and artificially soft screens provide very similar results. Indeed, in this region the artificially soft BC plays an important role since it is directly involved in the dominant diffraction mechanism. Both the relevant curves exhibit an attenuation which is much stronger (more than 10 dB) than that relevant to the *pec* TE_z case. In the third region, ($290° < \phi < 360°$), the curves relevant to the soft and the artificially soft cases deviate one from the other; there, indeed, the field is mainly influenced by the BC of the shadowed face, as can be inferred from the slope of the two TE_z curves. Nevertheless, the attenuation of the corrugated screen is always 10–15 dB higher than that of the *pec* screen for the same polarization.

In Figs. 3 and 4, numerical results from the high-frequency solution (continuous line) are found in a very good agreement with those from a MoM solution (dashed line). A $\lambda/4$-thick strip is considered, which has corrugations on both narrow sides, as depicted in the inset of the same figures. In particular, while a *pmc* face is adopted in the asymptotic solution, in the MoM model the actual corrugations are described by infinitely thin, $\lambda/20$ spaced teeth. A MoM Galerkin formulation is employed for solving the pertinent electric-field integral equation [20]. Piecewise sinusoidal, $\lambda/10$-wide basis/test functions have been used along the perimeter of the screen. For comparison, the same method is also applied to a thick screen without corrugations. The high-frequency results have been calculated by including all the double diffraction contributions. In Fig. 3, the total field is plotted from the lit to the dark region, for a 10λ-wide thick strip illuminated by a TE_z field. A magnetic line source is placed at $\rho_1' = 2\lambda$ from the leading edge and its angular coordinate from the lit face is 85°. In particular, it should be noted that in this case, at observation aspects close to $\phi = 270°$, the transition region of the first-order diffracted ray overlaps with that of the doubly diffracted ray. Again, in this case the attenuation introduced by the corrugations is considerable, despite of the small thickness. In Fig. 4, the shielding effects of a 2λ-wide thick strip are emphasized. There, a magnetic line source is placed on the axis of the strip, at $\lambda/4$ above the face. This example has been chosen because it may provide a 2-D model of a vertical dipole on a circular ground plane. This three-dimensional (3-D) geometry has been studied in [15] for the case in which the corrugation are etched on the lit face; this provided a drastic reduction of the sidelobe level. In the present case, it is found that the shadowing below the ground plane is significantly enhanced by the corrugations between the two edges.

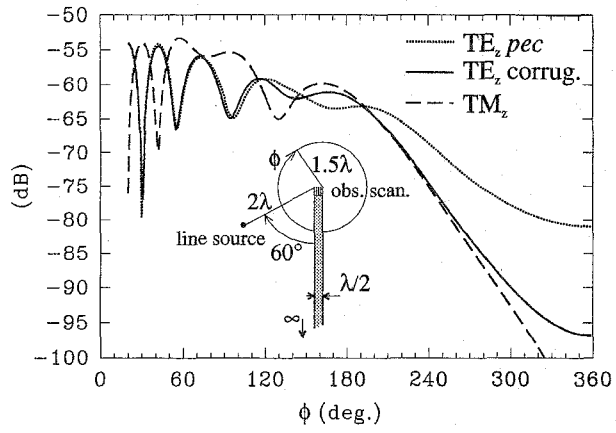

Fig. 2. High-frequency prediction of the amplitude of the total field for a semi-infinite thick screen with $\ell = \lambda/2$, dotted line *pec*-TE_z (hard), continuous line corrugated-TE_z (artificially soft), dashed line TM_z for both screens (soft).

It is worth pointing out that this excellent agreement between high-frequency and MoM results has been obtained for rather small values of the distance parameters. It should also be noted that our description involving diffraction mechanisms up to second order is, in general, very accurate except for almost unnoticeable discontinuities at the shadow boundaries of doubly diffracted fields. These minor inconveniences may be eliminated by introducing appropriate third-order diffracted field contributions.

The applicability of our solution to small thicknesses of the screen is further emphasized in Fig. 5. There, the total field for a TE_z illumination of either a smooth *pec* [Fig. 5(a)] or an artificially soft [Fig. 5(b)] top-thick edge is plotted for various

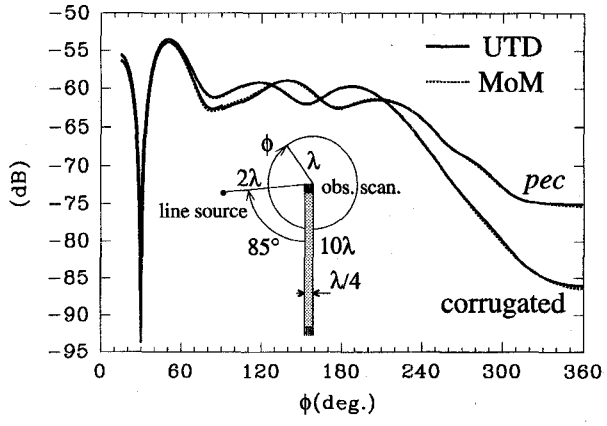

Fig. 3. Comparison between MoM (dotted line) and high-frequency (continuous line) results. Amplitude of the total field produced by a magnetic line source (TE_z), in the presence of a 10λ wide, $\lambda/4$-thick strip (near-grazing illumination).

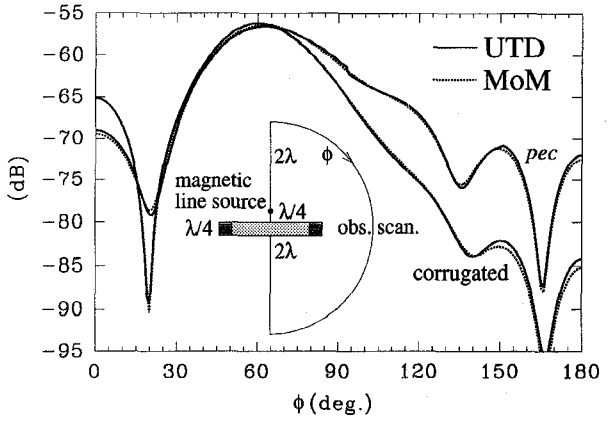

Fig. 4. Comparison between MoM (dotted line) and high-frequency (continuous line) results. Amplitude of the total field produced by a magnetic line source (TE_z) in presence of a 2λ-wide $\lambda/4$-thick strip.

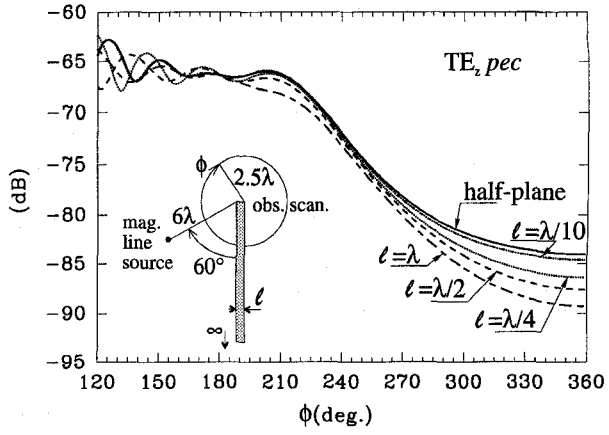

(a)

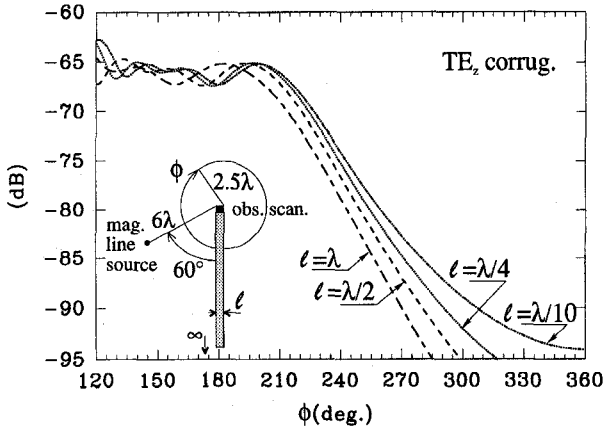

(b)

Fig. 5. Field of a magnetic line source placed at 6λ from the leading edge of a thick, either (a) *pec* or (b) artificially soft screen, for various thicknesses.

thicknesses. The example presented in Fig. 5(a) clearly shows that our high-frequency solution fails so gracefully that the results gradually blend into those obtained from the solution of the half-plane (continuous line). The same behavior is obtained for a TM_z illumination of the screen. This property provides a desirable degree of confidence on the robustness of this high-frequency solution which is found effective even for a vanishing distance between the double diffraction points. In comparing Fig. 5(a) with (b) it is noted that the shadowing effect produced by the corrugations is still significant, even for a quite thin screen, and dramatically increases for increasing thickness.

V. Concluding Remarks

A closed-form high-frequency solution has been presented for the scattering in the near zone by a thick screen that is illuminated by a source at a finite distance. The solution has been obtained by using a spectral cylindrical wave representation of the first-order diffracted field from the leading edge, together with an appropriate spectral response of the second edge. The cylindrical wave/near-field integral representation of the doubly diffracted field has been asymptotically evaluated to find the desired high-frequency expressions that involve appropriate transition functions. These transition functions, which are expressed in terms of the GFI, also properly account for the slope contribution of the primary diffraction; thus, they provide a suitable description of double diffraction mechanisms even when the two edges are joined by a soft or an artificially soft surface.

Numerical comparisons with an MoM solution have demonstrated the effectiveness of the present solution for calculating the field at any illumination and observation aspects including overlapping transition regions, even for moderate values of the distance parameters. It has been found that this high-frequency solution is applicable even for vanishing thickness of the screen. These same comparisons with the MoM solution for corrugated screens have also demonstrated the usefulness of the artificially soft boundary condition in modeling the corrugations.

Appendix

In this Appendix, the basic steps of the asymptotic evaluation of the integral in (12) are summarized. Let us denote each one of the four integrals in (12) by

$$I_{pq}^{h,a,s} = \int_{-j\infty}^{j\infty}\int_{-j\infty}^{j\infty} \frac{1}{4j} H_0^{(2)}(kR(\alpha_1,\alpha_2)) F_1^{h,a,s}(\Phi_1^p,\alpha_1) \cdot F_2^{h,a,s}(\Phi_2^q,\alpha_2)\, d\alpha_1\, d\alpha_2. \quad (24)$$

As mentioned in Section III, the integrand exhibits a 2-D saddle point at $(\alpha_1, \alpha_2) = (0,0)$, and the asymptotic evaluation is performed taking into account the nearest poles. Also, it is seen that in both the artificially soft (a) and the soft (s) cases, the integrand vanishes at the saddle point.

To asymptotically express (24) in terms of canonical integral forms, we multiply and divide the integrand by a suitable function which exhibits the same singularities and zeros. This function is the same as that occurring in the case of double diffraction by two edges in a planar surface which was treated in [12], i.e.,

$$Q^{h,a,s}(\alpha_1,\alpha_2) = \frac{q^{h,a,s}(\alpha_1,\alpha_2)}{\left(\sin^2\frac{\alpha_1}{2}-\sin^2\frac{\alpha_1^p}{2}\right)\left(\sin^2\frac{\alpha_2}{2}-\sin^2\frac{\alpha_2^q}{2}\right)} \tag{25}$$

where $q^h(\alpha_1,\alpha_2) = \sin(\alpha_1^p/2)\sin(\alpha_2^q/2)$ in the hard case, and $q^{a,s}(\alpha_1,\alpha_2) = \sin(\alpha_1/2)\sin(\alpha_2/2)$ in both the artificially soft and the soft cases. The ratio $C^{h,a,s}(\alpha_1,\alpha_2)$ between $F_1(\Phi_1^p,\alpha_1)F_2(\Phi_2^q,\alpha_2)$ and $Q^{h,a,s}(\alpha_1,\alpha_2)$ is a regular slowly varying function close to and at the 2-D saddle point. Next, the asymptotic approximation for large argument of the Hankel function is introduced. Then, the slowly varying term $C^{h,a,s}(\alpha_1,\alpha_2)/\sqrt{R(\alpha_1,\alpha_2)}$ is approximated by its value at the saddle point. Thus

$$I^{h,a,s} = \frac{1}{2\sqrt{2\pi jk}}\frac{1}{\sqrt{(\rho_1'+\ell+\rho_2)}}C^{h,a,s}(0,0)\int_{-j\infty}^{j\infty} \cdot \int_{-j\infty}^{j\infty} e^{-jkR(\alpha_1,\alpha_2)}Q^{h,a,s}(\alpha_1,\alpha_2)\,d\alpha_1\,d\alpha_2 \tag{26}$$

which is similar to that in [12], and is treated in the same fashion to yield (14).

REFERENCES

[1] S. A. Bokhari, M. Keer, and F. E. Gardiol, "Site shielding of earth-station antennas," *IEEE Antennas Propagat. Mag.*, vol. 37, no. 1, Feb. 1995.

[2] P.-S. Kildal, "Artificially soft and hard surfaces in electromagnetics," *IEEE Trans. Antennas Propagat.*, vol. 38, pp. 1537–1544, Oct. 1990.

[3] G. L. James and G. D. Poulton, "Double knife-edge diffraction for curved screens," *Microwaves, Opt., Acoust.*, vol. 3, pp. 221–223, Nov. 1979.

[4] R. Tiberio and R. G. Kouyoumjian, "A uniform GTD solution for the diffraction by strips illuminated at grazing incidence," *Radio Sci.*, vol. 14, pp. 933–941, 1979.

[5] ——, "An analysis of diffraction at edges illuminated by transition region fields," *Radio Sci.* vol. 17, pp. 323–336, 1982.

[6] R. Tiberio, G. Manara, G. Pelosi, and R. Kouyoumjian, "High-frequency electromagnetic scattering of plane waves from double wedges," *IEEE Trans. Antennas Propagat.*, vol. 37, pp. 1172–1180, Sept. 1989.

[7] M. Schneider and R. Luebbers "A general UTD diffraction coefficient for two wedges," *IEEE Trans. Antennas Propagat.* vol. 39, pp. 8–14, Jan. 1991.

[8] A. Michaeli "A new, asymptotic high-frequency analysis of electromagnetic scattering by a pair of parallel edges—Closed form results," *Radio Sci.* vol. 20, pp. 1537–1548, 1985.

[9] A. Michaeli "A hybrid asymptotic solution for the scattering by a pair of perfectly conducting wedges," *IEEE Trans. Antennas Propagat.*, vol. 38, pp. 664–667, May 1990.

[10] L. P. Ivrissimtzis and R. J. Marhefka, "Double diffraction at a coplanar skewed edge configuration," *Radio Sci.*, vol. 26, pp. 821–830, 1991.

[11] ——, "A uniform ray approximation of the scattering by polyhedral structures including higher terms," *IEEE Trans. Antennas Propagat.*, vol. 40, pp. 1302–1312, Nov. 1992.

[12] M. Albani, F. Capolino, S. Maci, and R. Tiberio, "Double diffraction coefficients for source and observation at finite distance for a pair of wedges," presented at *IEEE AP-S Symp.*, Newport Beach, CA, June 1995 (also, *IEEE Trans. Antennas Propagat.*, to be published).

[13] R. G. Kouyoumjian and P. H. Pathak, "A uniform geometrical theory of diffraction for an edge in a perfectly conducting surface," *Proc. IEEE* vol. 62, pp. 1448–1461, Nov. 1974.

[14] S. Maci, R. Tiberio, and A. Toccafondi, "Diffraction coefficient for artificially soft and hard surfaces," *Electron. Lett.*, vol. 30, no. 3, pp. 203–204, Feb. 1994.

[15] M. Leoncini, S. Maci, and A. Toccafondi, "Analysis of the electromagnetic scattering by artificially soft discs," *IEE Proc. H,* vol. 142, no. 5, pp. 399–404, Oct. 1995.

[16] D. S. Jones, "A uniform asymptotic expansion of a certain double integral," *Proc. Royal Soc. Edinburgh (A)*, vol. 69, no. 15, pp. 205–226, 1971.

[17] P. C. Clemmow and T. B. A. Senior, "A note on the generalized Fresnel integral," *Proc. Cambridge Phil. Soc.*, vol. 49, pp. 570–572, 1953.

[18] L. Felsen and N. Marcuvitz, *Radiation and Scattering of Waves.* Englewood Cliffs, NJ: Prentice-Hall, 1973 (reprinted *Ser. Electromagn. Waves.* Piscataway, NJ: IEEE Press, 1994).

[19] F. Capolino and S. Maci, "Simplified, closed-form expressions for computing the generalized Fresnel integral and their application to vertex diffraction," *Microwave Opt. Tech. Lett.*, vol. 9, no. 1, pp. 32–37, May 1995.

[20] R. F. Harrington, *Field Computation by Moment Methods*, 2nd ed. New York: IEEE Press, 1992.

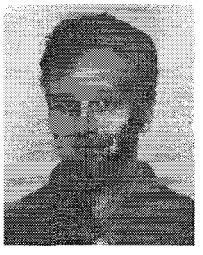

Matteo Albani was born in Florence, Italy, in 1970. He received the doctor degree (*cum laude*) in electronic engineering from the University of Florence, Italy, in 1994. He is currently involved in a Ph.D. research program at the University of Siena, Italy.

His research interests are focused on high-frequency methods for electromagnetics.

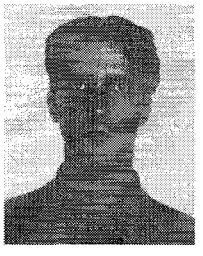

Filippo Capolino (S'94) was born in Florence, Italy, in 1967. He received the doctor degree (*cum laude*) in electronic engineering from the University of Florence, Italy, in 1993, where he is presently involved with a Ph.D. research program.

Since 1994, he has been an Instructor at the University of Siena, Italy. His main research interests are with theoretical and applied electromagnetics, in particular with high-frequency methods for electromagnetic scattering and electromagnetic models of random surfaces.

Dr. Capolino received an award at the MMET 1994 Student Paper Competition, and in 1996 he won the Raj Mittra Travel Grant for Young Scientists.

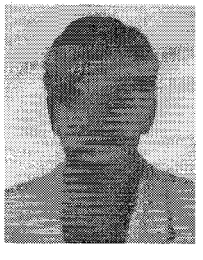

Stefano Maci (M'92) was born in Rome, Italy, in 1961. He received the doctor degree in electronic engineering from the University of Florence, Italy, in 1987.

In 1990, he joined the Department of Electronic Engineering of the University of Florence, Italy, as an Assistant Professor. Since 1993, he has also been an Adjunct Professor at the University of Siena, Italy. His main interest is electromagnetic theory, mainly concerning high- and low-frequency methods for antennas and electromagnetic scattering. He has also developed a research activity on specific topics concerning microwave antennas, particularly focused on the analysis, synthesis, and design of patch antennas.

Dr. Maci won the national "Francini" Award for Young Scientists in 1988.

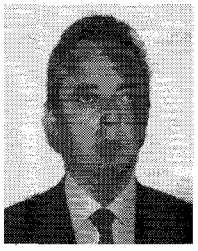

Roberto Tiberio (M'81–SM'91–F'93) was born in Rome, Italy, in 1946. He received the doctor degree (*cum laude*) from the University of Pisa, Italy, in 1970.

In 1972, he joined the Department of Electronic Engineering of the University of Florence, Italy, where he has been Full Professor since October 1993. After 1972 he joined the University of Siena, Italy, where he is currently the Dean of the College of Engineering. Since 1976 he has been collaborating with the Electroscience Laboratory of the Ohio State University, Columbus, where he worked continuously as a Senior Research Associate for two years, and then, periodically, as a Scientific Consultant. His research interests are focused on electromagnetic theory and high-frequency methods, mainly concerning the development and applications of analytic and numerical techniques for antenna design and RCS prediction.

Dr. Tiberio is an Italian Delegate of URSI Commission B.